Cell, Vol. 122, 97–106, July 15, 2005, Copyright ©2005 by Elsevier Inc. DOI 10.1016/j.cell.2005.04.033

Dynein Anchors Its mRNA Cargo after Apical Transport in the *Drosophila* Blastoderm Embryo

Renald Delanoue and Ilan Davis*
Wellcome Trust Centre for Cell Biology
School of Biological Sciences
The University of Edinburgh
Edinburgh EH9 3JR
United Kingdom

Summary

Molecular motors actively transport many types of cargo along the cytoskeleton in a wide range of organisms. One class of cargo is localized mRNAs, which are transported by myosin on actin filaments or by kinesin and dynein on microtubules. How the cargo is kept at its final intracellular destination and whether the motors are recycled after completion of transport are poorly understood. Here, we use a new RNA anchoring assay in living *Drosophila* blastoderm embryos to show that apical anchoring of mRNA after completion of dynein transport does not depend on actin or on continuous active transport by the motor. Instead, apical anchoring of RNA requires microtubules and involves dynein as a static anchor that remains with the cargo at its final destination. We propose a general principle that could also apply to other dynein cargo and to some other molecular motors, whereby cargo transport and anchoring reside in the same molecule.

Introduction

Intracellular mRNA localization is a universal posttranscriptional mode of targeting proteins to their site of function (Lopez de Heredia and Jansen, 2004; Van de Bor and Davis, 2004). Examples are known in most model organisms, ranging from yeast to mammals, and include mRNAs encoding a diverse range of proteins (Palacios and St Johnston, 2001). The most common mechanism of sorting mRNAs in the cytoplasm is probably transport by molecular motors (Tekotte and Davis, 2002). Such motors are large multicomplex molecular machines that use ATP hydrolysis to transport cargo in a directed manner along microtubules (MTs) or actin (Vale, 2003). Well-studied examples include myosin-dependent transport of *ASH1* mRNA in yeast (Bertrand et al., 1998; Takizawa et al., 1997) and kinesin I-dependent transport of *oskar* (*osk*) mRNA to the plus ends of MTs in *Drosophila* (Brendza et al., 2000; Palacios and St Johnston, 2002).

Another RNA cargo transported by a molecular motor is *grk* mRNA, which encodes a TGF-α protein. The Grk signal acts twice during oogenesis, first to initiate the anteroposterior axis and later to initiate the dorsoventral axis (Gonzalez-Reyes et al., 1995; Neuman-Silberberg and Schüpbach, 1993). The minus end directed MT motor cytoplasmic dynein (dynein) transports *gurken (grk)* mRNA (Duncan and Warrior, 2002; MacDougall et al., 2003) to a dorsoanterior cap near the oocyte nucleus. This transport occurs in two steps, each of which probably involves distinct networks of MTs (MacDougall et al., 2003). *bicoid* (*bcd*) mRNA probably also requires dynein for its localization in the oocyte, as an excess of p50/dynamitin, part of the Dynactin, a dynein-associated complex required for its processivity, disrupts *bcd* mRNA localization (Duncan and Warrior, 2002; Januschke et al., 2002). This idea is supported by the fact that, Swallow, a factor required for *bcd* mRNA localization (St Johnston et al., 1989; Stephenson et al., 1988) interacts by two hybrid with dynein light chain (Schnorrer et al., 2000). Dynein also transports *wingless* (*wg*) and pair-rule mRNA to the apical cytoplasm of blastoderm embryos (Bullock and Ish-Horowicz, 2001; Wilkie and Davis, 2001). Apical mRNA localization targets the Wg (WNT) signal apically (Simmonds et al., 2001) and is important for the accuracy of segmentation (Bullock et al., 2004). Injected fluorescently labeled pair-rule or *wg*, RNA assembles into particles whose apical localization can be followed in living embryos (Wilkie and Davis, 2001). In many cases, endogenous mRNAs also localize as particles, which are believed to consist of many RNA molecules complexed with molecular motors and their cofactors (Ferrandon et al., 1994; Kanai et al., 2004; Wagner et al., 2001). Use of the injection assay has revealed that the apical transport of *wg* and pair-rule RNA require MTs but not actin and depends on dynein and its associated dynactin complex (Wilkie and Davis, 2001). Injected pair-rule RNA recruits the dynein cofactors, Egalitarian (Egl) and Bicaudal D (BicD) (Bullock and Ish-Horowicz, 2001), which are also required for apical transport of pair-rule mRNA (Bullock and Ish-Horowicz, 2001). BicD and Egl were previously shown to bind to each other and to be required for oocyte determination (Mach and Lehmann, 1997). In mammalian cells, BicD has been shown to bind to dynein and is perhaps involved in cargo recognition (Hoogenraad et al., 2001; Matanis et al., 2002). In *Drosophila*, Egl has been shown to bind to dynein light chain (Dlc), a dynein motor component, through an Egl domain distinct from its BicD binding domain (Navarro et al., 2004).

After being transported, specific transcripts must be kept at their site of localization. Although several molecular motors, adaptors, and *trans*-acting factors involved in the movement of mRNAs in a number of different systems have been identified; surprisingly, little is known about RNA anchoring. In a few specific cases, actin has been implicated in RNA anchoring, although this has not been directly demonstrated. For example, in addition to requiring kinesin for its transport, *osk* mRNA is thought to be anchored in an actin-dependent manner. *osk* mRNA localization also requires the actin associated proteins, Moesin and Tropomyosin (Erdelyi et al., 1995; Glotzer et al., 1997; Jankovics et al., 2002), as well as *bifocal*, which may act as actin-dependent anchors (Babu et al., 2004). The maintenance of yeast *ASH1* mRNA localization to the bud involves Bud6p/

*Correspondence: ilan.davis@ed.ac.uk

Aip3p and Bni1p/She5p, proteins required for actin organization and the establishment of polarity (Beach et al., 1999). In chicken fibroblasts, the movement and anchoring of β-actin mRNA requires F-actin but not MTs (Latham et al., 2001; Sundell and Singer, 1991), whereas *Vg1* mRNA localization in *Xenopus* oocytes requires both MTs and actin (Yisraeli et al., 1990). In some of these examples, it is thought that RNA is tethered at the site of localization by a static actin-based anchor, when the RNA is released from the motor. However, in the case of dynein-dependent mRNA transport, there is no evidence of a role for actin in anchoring and it is not known how dynein cargo is retained at its final destination. Nor is it known whether the dynein motor protein complex releases the RNA cargo at the final destination and then participates in further rounds of transport. In general, the various alternative hypotheses for how RNA localization can be maintained after transport have not been tested directly.

Results

MTs, and Not Actin, Are Required for Apical RNA Anchoring

We have developed a specific assay to distinguish between a number of possible hypotheses (see Discussion) for how RNA localization can be maintained after transport. Injected *wg, runt* (*run*), and *fushi tarazu (ftz)* RNA (Bullock and Ish-Horowicz, 2001; Wilkie and Davis, 2001) fluorescently tagged with AlexaFluor546 (red), were allowed to fully localize before injection of cytoskeletal inhibitors and other reagents previously shown to interfere with the dynein motor or its associated factors.

We first investigated whether actin is required for apical anchoring of RNA in the blastoderm embryo by allowing injected RNA to fully localize and then injecting the actin polymerization inhibitor, LatrunculinA. Injection of 10 mM LatrunculinA disrupts the actin network completely (within the limits of fluorescent detection) and disrupts the apical position of nuclei, which is actin dependent (Figures 1A–1D; Edgar et al., 1987). However, *wg* and pair-rule RNA remain tightly associated with the displaced nuclei (Figures 1E and 1F; see Movie S1 in the Supplemental Data available with this article online). Moreover, injecting LatrunculinA before the fluorescent RNA does not prevent the active transport of the RNA to internalized nuclei (Wilkie and Davis, 2001) nor the anchoring of RNA near the nuclei (Figures 1G and 1H; Movie S2). We conclude that like the active transport of pair-rule and *wg* RNA, their apical anchoring does not require F-actin.

We then investigated whether MTs are required for apical anchoring of RNA following its transport by performing similar experiments with Colcemid or Nocodazole, drugs that prevent MT polymerization. We found that disrupting the MTs in early interphase 14 blastoderm embryos causes the rapid mislocalization of apical RNA (Figures 2A and 2B; Movie S3); whereas in control embryos injected with water or buffer, apical RNA localization is maintained for long periods (data not shown). MTs are distributed in an apical cap surrounding each nucleus in the syncytial blastoderm embryo

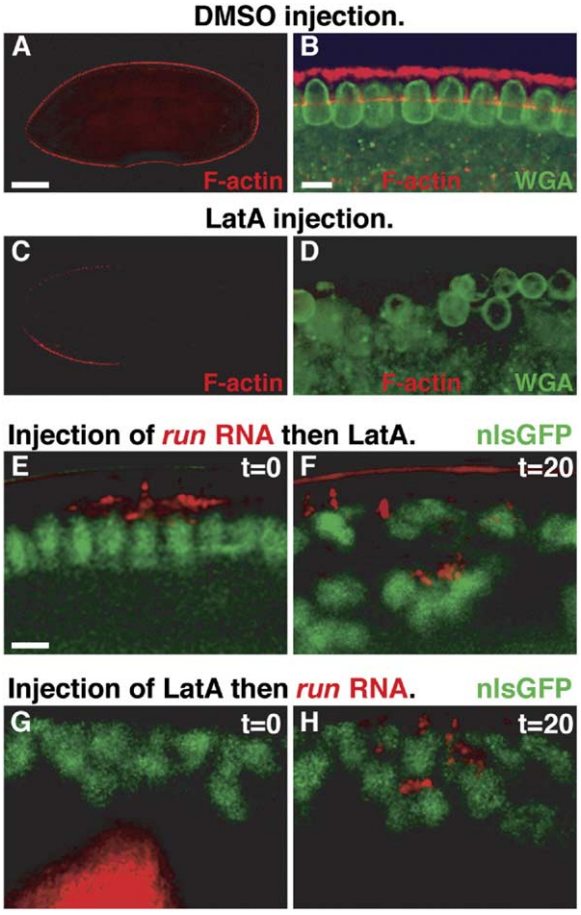

Figure 1. F-actin Is Not Required for Anchoring Apical Transcripts

(A and B) Cortical actin (phalloidin-AlexaFluor568, in red) is normal in a control DMSO-injected embryo. Nuclear envelope is shown in green (wheat germ agglutinin-AlexaFluor488).

(A) Low magnification.

(B) High magnification showing cortical actin and actin at the elongating membrane furrows above the coaligned nuclei.

(C) LatrunculinA (10 mM) injection at the posterior of a blastoderm embryo causes depolymerization of actin (red).

(D) LatrunculinA (10 mM) injection also causes loss of cortical anchoring of nuclei (green).

(E and F) Two time points from a time lapse movie of blastoderm embryo, expressing the nuclear marker nlsGFP fusion protein (green) and preinjected with AlexaFluor548-labeled *run* RNA, which is fully localized (red).

(E) At t = 0 min (10 min after RNA injection), LatrunculinA is injected.

(F) At t = 20 min, the injected RNA remains tightly associated with the displaced nuclei, which lack actin.

(G and H) Two time points from time lapse movie of nlsGFP (green) blastoderm embryo preinjected with LatrunculinA (10 mM).

(G) At t = 0 min (10 min after LatrunculinA injection), AlexaFluor548-labeled *run* RNA was injected (red).

(H) At t = 20 min, the RNA is localized and anchors next to the internally displaced nuclei devoid of F-actin.

Scale bars are 100 μm (A and C) and 10 μm (B, D, and E–H). In (B), (D), (E)–(H) and all subsequent figures, apical is up and basal is down.

(Foe et al., 1993; Figure 2C). To test whether MTs are also present in internalized nuclei of embryos with depolymerized F-actin, we fixed embryos 10 min after

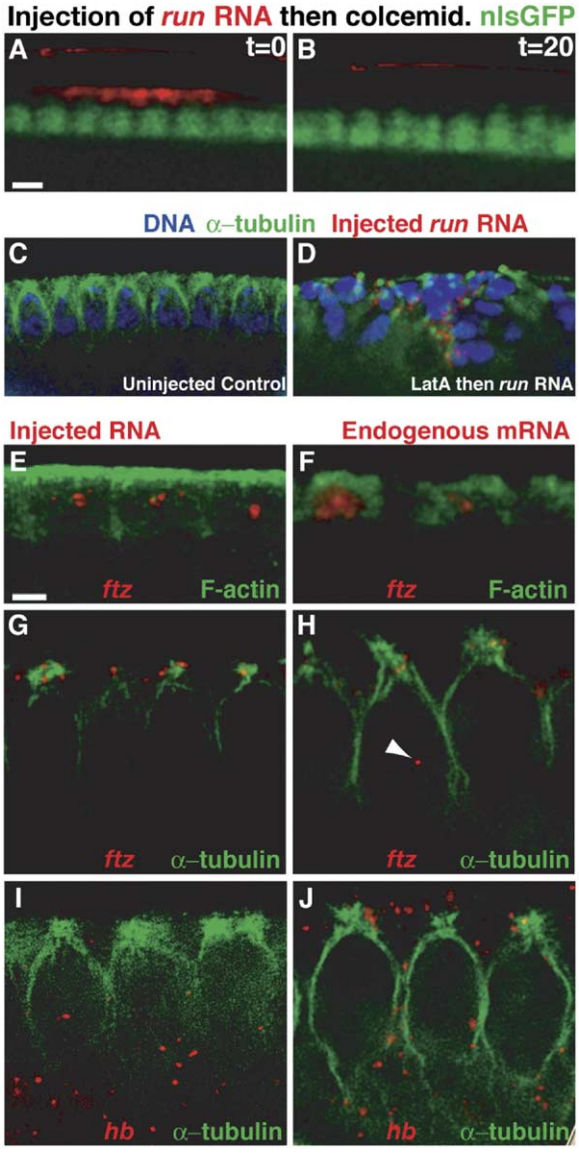

Figure 2. MTs Are Required for Anchoring Apical Transcripts

(A and B) Two snapshots from a time lapse movie of nlsGFP (green) embryo preinjected with AlexaFluor546-labeled RNA (red).

(A) At t = 0 min (10 min after RNA injection), Colcemid (100 μg/ml) is injected into the embryo.

(B) After 20 min, RNA is no longer apically localized.

(C) MTs organization shown by anti-α-tubulin staining (green) relative to coaligned nuclei (blue).

(D) Blastoderm embryo injected with LatrunculinA (10 mM) and biotin-labeled *run* then fixed and stained for MTs. Internalized nuclei (blue) retain some MTs (green) and the injected *run* RNA (streptavidin AlexaFluor568 in red) is able to localize to these nuclei.

(E and F) Injected *ftz* RNA (E) and endogenous *ftz* mRNA detected by in situ hybridization (F) (red) localize underneath the cortical actin stained by phalloidin FITC (green).

(G) Almost all injected biotin-labeled *ftz* RNA particles (red) are localized near the apical MTs (anti-α-tubulin antibody, in green).

(H) Almost all of the endogenous *ftz* RNA particles (red) are localized on the MTs, next to the MT organizing center (MTOC). Bright signal within the nucleus is a nascent transcript focus (arrowhead).

(I and J) Injected (I) and endogenous *hb* RNA (J) do not colocalize with the MTs.

Scale bars are 10 μm (A–D) and 1 μm (E–J).

coinjecting LatrunculinA with pair-rule RNA and detected MTs with anti-α-tubulin antibody. We found that internalized nuclei retain some of their MTs, suggesting that MTs could be responsible for anchoring the RNA on internalized nuclei (Figure 2D).

If MTs, rather than actin, are required directly for apical anchoring of RNA, then RNA is likely to colocalize with MTs but not with actin. We tested this prediction by covisualizing endogenous or injected RNA with the cytoskeleton. Both injected and endogenous transcripts accumulate above the nuclei, but some distance from the cortical actin (Figures 2E, 2F, and S1A). In contrast, the vast majority of the injected and endogenous apical RNA is colocalized with MTs in the apical cytoplasm (Figures 2G, 2H, S1B, and S1D). In contrast, control injected or endogenous RNA of the gap gene *hunchback* (*hb*), previously shown to be unlocalized (Davis and Ish-Horowicz, 1991), only shows a low percentage of colocalization with MTs (Figures 2I, 2J, and S1C), consistent with chance colocalization in a relatively small volume of cytoplasm containing a dense network of MTs. Detailed statistical analysis shows that there are highly significant differences between the distances of apical versus unlocalized RNA particles and MTs (Figure S1E). We conclude that RNA is retained in the apical cytoplasm by an MT-dependent process and not by actin-dependent anchoring.

Apical RNA is localized above the nuclei, where the centrosomes and MT minus ends are also located (Callaini and Anselmi, 1988). Interestingly, the centrosome has been implicated in the localization of some RNAs (Lambert and Nagy, 2002; Schnorrer et al., 2002). We therefore covisualized both injected and endogenous RNA relative to γ-tubulin and tested its role in apical mRNA localization in the embryo. The results show that apical RNA is not colocalized with γ-tubulin (Figures S2A and S2B) nor to the broader pericentriolar region, revealed by anti-Centrosomin (Cnn) antibody (Figures S2C and S2D). Hypomorphic alleles of *γ-Tubulin37C* showed defects in anchoring of nuclei to the surface but showed no defects in apical mRNA localization (Figure S2E). We conclude that the centrosome is unlikely to play a major role in apical RNA anchoring.

Dynein Is Colocalized with Its RNA Cargo in the Apical Cytoplasm and Is Required for Maintenance of Apical RNA Localization

To determine whether dynein is required for retaining the RNA cargo following its apical transport, we used antibodies against components of the dynein complex, previously shown to disrupt dynein function in vivo (Sharp et al., 2000; Steffen et al., 1997; Wilkie and Davis, 2001). We found that injection of anti-dynein heavy chain (anti-Dhc) or anti-dynein intermediate chain (anti-Dic) antibodies after the RNA is fully localized causes a rapid disruption of apical localization (Figures 3A–3C and S3A and S3B; Movie S4). Similarly, endogenous apical RNA becomes unlocalized after injection of anti-Dhc antibody and can be observed deep in the basal cytoplasm and yolk, without affecting MT organization (Figures 3D–3F). These observations show that, like for injected RNA, the anchoring of endogenous RNA particles on the apical MTs requires the dy-

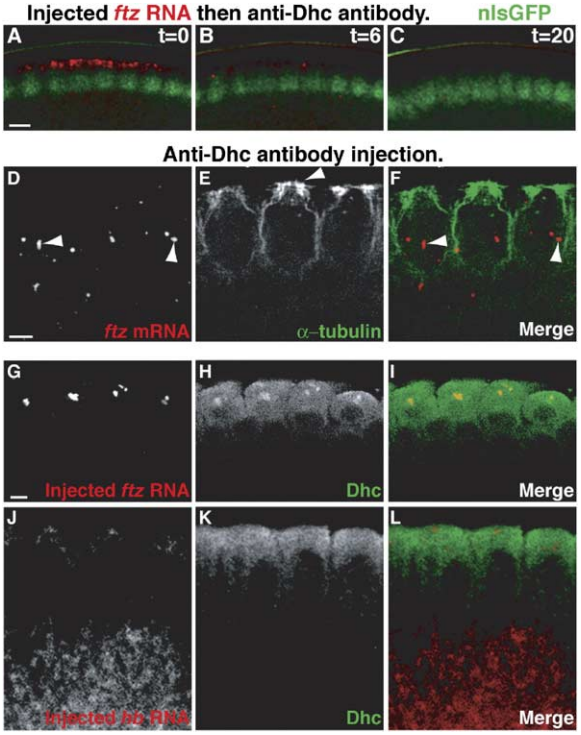

Figure 3. Maintenance of Apically Localized RNA Requires Dynein

(A–C) Three time points from a time lapse movie of an embryo showing that the apical localization of preinjected AlexaFluor546-labeled *ftz* RNA (red) is disrupted by injection of anti-Dhc antibody 10 min after the RNA.

(A) At t = 0 min, anti-Dhc antibody injected.

(B) At t = 6 min, most of the apical RNA has diffused away.

(C) t = 20 min, no apical RNA remains.

(D–F) Anti-Dhc antibody injection disrupts anchoring of endogenous apical RNA.

(D) In situ hybridization showing disruption of apical localization of endogenous *ftz* transcripts by injection of anti-Dhc antibody 15–20 min prior to fixation. Nascent transcript foci are indicated by arrowheads (E) MTs (anti-α-tubulin staining). Arrowhead shows representative apical MTOC.

(F) Merged image (compare with Figure 2H).

(G–I) Confocal sections show Dhc enrichment at the site of apical RNA localization.

(G) Injected biotinylated *ftz* RNA detected with Avidin AlexaFluor568 (red).

(H) Anti-Dhc antibody (green).

(I) Merged image.

(J–L) Injected biotinylated *hb* RNA detected with Avidin AlexaFluor568 (red) (J) does not recruit Dhc (K).

(L) Merged image.

Scale bars are 10 μm (A–C) and 1 μm (D–L).

nein motor. In contrast, anti-Dhc antibody injections have no effect on the distribution of either endogenous or injected unlocalized *hb* RNA (Figures S3C–S3F). We also showed that injection of the anti-Dhc antibody affects RNA anchoring on displaced nuclei after disruption of the actin network (Figures S3G and S3H). We conclude that dynein is required either directly or indirectly for the retention of endogenous and injected RNA in the apical cytoplasm after its transport.

A direct role for dynein in maintaining the localization of apical RNA would predict that the motor should be present with its RNA cargo in the apical cytoplasm. To test this prediction, we injected biotinylated pair-rule RNA, allowed it to fully localize for 10 min, and then fixed and covisualized dynein and RNA in the embryo. The results show that some dynein becomes enriched with the apical RNA at its site of localization (Figures 3H and 3I). These sites are not found in the absence of RNA injection and are distinct from the majority of dynein in the embryo, which remains ubiquitously distributed with some general apical enrichment. In contrast, when unlocalized *hb* RNA is injected basally and diffuses to all parts of the cytoplasm, including apically, it does not recruit dynein to the unlocalized RNA particles (Figures 3J–3L). We also found that p50/Dynamitin (Dmn), a subunit of the dynactin complex, is enriched with the apically localized RNA (Figure S4). We conclude that dynein is required directly to maintain RNA at its apical destination.

Dynein Acts as a Static RNA Anchor, Independently of Its Transport Activity

The results so far suggest two possible models for how dynein could act to retain RNA in the apical cytoplasm. Dynein could be required to continuously and actively transport RNA to the apical cytoplasm. Such dynamic maintenance of RNA localization would involve the motor detaching from the MTs with or without the cargo, once it arrives at its apical destination. The cargo would then diffuse away from the site of localization and have to be retransported by newly captured dynein motors. The second possible model is that dynein could act as a static anchor that links the cargo to the MTs once it reaches its apical destination (see Discussion for models). We used a number of complementary approaches to distinguish between these two possibilities by testing whether apical retention of RNA requires dynein-dependent active transport.

One prediction of the continuous active transport model is that factors required for the activity of the dynein motor during apical transport should also be required for apical retention of RNA. These include the ATPase activity of the motor as well as its cofactors BicD and Egl (Bullock and Ish-Horowicz, 2001). We first preinjected embryos with an ATPase inhibitor, the sodium orthovanadate (Vanadate), at concentrations previously shown to disrupt dynein function in vitro (Gordon, 1991). Under these conditions, active apical transport of RNA is completely inhibited (Figures 4A–4C; Movie S5). In contrast, Vanadate has no effect on the retention of RNA already transported apically (Figures 4D–4F; Movie S6). In order to test whether apical RNA anchoring occurs by the normal mechanism even in the presence of Vanadate, we injected anti-Dhc antibody 10 min after Vanadate was injected. The results show that anti-Dhc antibody disrupts apical anchoring in the presence of Vanadate, suggesting that Vanadate does not bypass the normal requirement for dynein in anchoring (Figures 4G–4I).

Our results with injected RNA predict that inhibiting ATPase-dependant dynein transport with Vanadate should lead to the accumulation of endogenous pair-rule and *wg* transcripts in the basal cytoplasm. They also predict that some RNA particles will remain api-

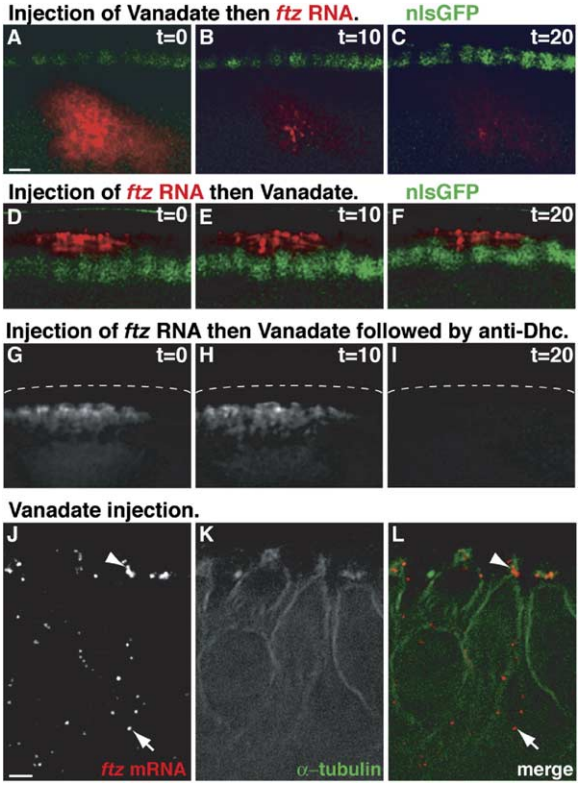

Figure 4. Apical RNA Requires the Motor for Anchoring but Not Its ATPase Activity

(A–C) Three time lapse images from a movie showing inhibition of apical RNA transport by Vanadate (10 mM) preinjection (10 min before RNA).

(A) t = 0 min, (B), t = 10 min, and (C) t = 20 min after injection of AlexaFluor546-labeled *ftz* RNA (red).

(D–F) Three time lapse images from a movie showing that Vanadate (10 mM) injection (at t = 0 min) does not disrupt apical anchoring of preinjected (10 min before Vanadate) AlexaFluor546-labeled *ftz* RNA (red).

(G–I) Three snapshots of a time lapse movie showing an embryo preinjected with an AlexaFluor546 *ftz* RNA.

(G) At t = 0 min, Vanadate (10 mM) was injected with no effect on RNA localization (H). At t = 10 min, the anti-Dhc antibody was injected (H) causing a disruption of RNA anchoring (I). Dotted line indicates the plasma membrane.

(J–L) In situ hybridization showing a disruption of endogenous *ftz* mRNA localization by injection of Vanadate (10 mM) 15–20 min prior to fixation.

(J) Some endogenous *ftz* transcripts remain anchored (arrowhead) but many untransported *ftz* particles accumulate in the basal cytoplasm (arrow).

(K) Anti-α-tubulin antibody (green), showing partly disorganized MTs caused by Vanadate injection, which do not disrupt RNA anchoring.

(L) Merged image (compare with Figure 3F).

Scale bars are 10 μm (A–I) and 1 μm (J–L).

cally localized if anchoring is unaffected by Vanadate. We tested these predictions by injecting Vanadate into embryos, fixing them 15–20 min later, and assaying the localization of the endogenous transcripts. The results show a partial mislocalization phenotype, as predicted (Figures 4J–4L). We interpret these results as indicating that newly synthesized transcripts after the injection of Vanadate fail to localize because of inhibition of the ATPase activity of dynein, but RNA that was anchored before the Vanadate injection remains apically localized. We conclude that the ATPase function of dynein is not required for the motor to maintain the apical localization of RNA, despite being required for its transport.

BicD and Egl were previously shown to be recruited by injected pair-rule mRNA and to be essential for apical mRNA transport (Bullock and Ish-Horowicz, 2001). We tested whether BicD and Egl are also required for apical anchoring of mRNA (Bullock and Ish-Horowicz, 2001). We were able to distinguish in the same embryo between RNA that is anchored and RNA that is being transported by first injecting red *run* RNA and allowing it to localize fully. Ten minutes later, we coinjected Egl antibody with red *run* RNA. The results show that Egl antibody prevents the localization of the coinjected green RNA but does not affect the distribution of prelocalized red RNA (Figures 5A–5C; Movie S7). We obtained similar results irrespective of the order of injection of red and green RNA or using an anti-BicD antibody, and in control experiments, consecutive injections of the two RNAs lead to both localizing apically (data not shown). A further injection of anti-Dhc antibody, 10 min after anti-Egl antibody injection into embryos with prelocalized RNA, disrupts apical retention of RNA (Figures 5D–5F), excluding the possibility that the anti-Egl antibody acts by crosslinking the RNP complex in the apical cytoplasm.

Our results with injected RNA predict that endogenous apical RNA anchoring is Egl and BicD independent. We tested this prediction by injecting anti-Egl and anti-BicD antibodies, fixing the embryos 15–20 min later, and performing in situ hybridization with probes against pair-rule genes. Our results show that disrupting Egl or BicD function causes a partial mislocalization of the endogenous apical transcripts (Figures 5G–5I and data not shown). We interpret the partial mislocalization as follows: RNA that was localized before the injection of the antibodies remained anchored and RNA that is newly synthesized after the injection of antibody is unable to localize. Our interpretation is supported by the fact that we also observed that injected anti-Egl antibody prevents the apical movement of RNA particles in the middle of their apical transport (Movie S8), showing that the antibody acts by disrupting Egl function in apical transport, rather than preventing the assembly of a transport-competent RNP complex. Furthermore, we also confirmed that the anti-Egl antibody is able to recognize and bind Egl when apically localized within the motor-cargo complex. We injected RNA, allowed it to localize apically for 10 min, and then injected the anti-Egl antibody and waited 20 min before fixing the embryos. The results show that the anti-Egl antibody is enriched with the anchored RNA. Therefore, the anti-Egl antibody is able to bind and to disrupt efficiently the Egl protein associated with apically localized RNA in living embryos (Figures 5J–5L). Moreover, we show that in such embryos BicD is also enriched in the same site (Figure 5M). We conclude that BicD and Egl are required for active transport of RNA, but not for dynein-dependent retention of apical RNA.

To further test whether BicD and Egl remain with the

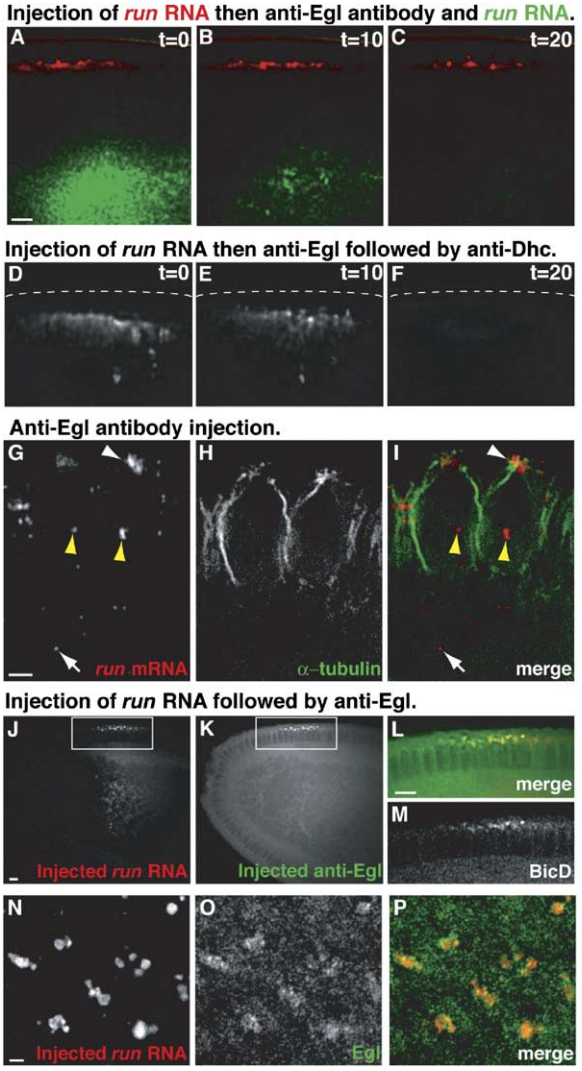

Figure 5. Apical RNA Anchoring Is Independent of BicD and Egl

(A–C) Three time lapse images from a movie of an embryo preinjected with AlexaFluor546-labeled *run* RNA (red), 10 min before coinjection ([A], at t = 0 min) of anti-Egl antibody and AlexaFluor488-labeled *run* RNA (green).

(C) After 20 min, green *run* RNA is unlocalized, but the anchoring of the red *run* RNA is not affected.

(D–F) Snapshots of a time lapse movie showing a preinjected embryo with an AlexaFluor546 *run* RNA.

(D) The anti-Egl antibody is injected with no effect on the apical RNA anchoring (E).

(E) At t = 10 min, the anti-Dhc antibody is injected and removes the apically localized RNA.

(F) Dotted line indicates the plasma membrane.

(G–I) In situ hybridization showing that some endogenous *run* mRNA (G) accumulates basally (arrow), while other *run* mRNA remains anchored apically (arrowhead) after anti-Egl antibody injection (15–20 min prior to fixation). Yellow arrowheads show nascent transcript foci.

(H) Anti-α-tubulin antibody (green).

(I) Merged image (compare with Figure 3F).

(J–M) Embryo preinjected with biotinylated *run* RNA and then injected 10 min later with the anti-Egl antibody and fixed 20 min later.

(J) RNA visualized with Avidin AlexaFluor568.

(K) Anti-Egl detected by an anti-rabbit AlexaFluor488 antibody.

(L) Inset of the merged image.

(M) Anti-BicD, detected with cy5 secondary antibody, showing the presence of BicD with the same apically anchored RNA.

(N–P) Apical view of an embryo fixed 20 min after injection with a biotin-labeled *run* RNA showing colocalization with Egl.

(N) RNA is detected with Avidin AlexaFluor568 (red).

(O) Anti-Egl antibody (green).

(P) Merged image.

Scale bars are 10 μm (A–F and J–M) and 1 μm (G–I and N–P).

dynein-cargo complex when it arrives at the apical destination, we injected RNA, allowed it to fully localize, and covisualized it with Egl or BicD after fixation. The results show that Egl and BicD are colocalized with the RNA in the apical cytoplasm next to peripheral nuclei (Figures 5N–5P and data not shown). This enrichment of BicD and Egl is dependent on the presence of RNA and is likely to be due to the movement of the proteins with the RNA from the basal cytoplasm. We conclude that BicD and Egl are present with the dynein-cargo complex at the final apical site of localization, despite not being required for retention at this site.

Another prediction of the continuous active transport model is that a reduction in the activity of dynein would lead to a reduced efficiency of apical retention of RNA. We tested this prediction in a number of independent ways: using *p50/dynamitin* overexpression that disrupts the dynein processivity factor dynactin, a dominant mutant in another component of the dynactin complex, *Glued*[1], and by using *dynein* and *BicD* mutants. We previously showed that RNA is transported at slower speeds in *dhc* mutants (Wilkie and Davis, 2001), and we also found a statistically highly significant reduction in the speed of RNA transport in *Glued*[1] and *BicD* mutants (Table S1). However, we observed no change in the degree to which injected RNA is retained at the apical cytoplasm after transport (Figure S5), despite some endogenous unlocalized transcripts being present basally (Figure S5). We conclude that a reduction in the speed of apical transport does not affect the efficiency of apical retention of RNA.

A third prediction of the continuous active transport model is that RNA particles should be visible in the apical cytoplasm in continuous apical flux. To test this prediction, we covisualized the apically localized RNA with the nuclei at high resolution in three dimensions. While there are substantial cytoplasmic movements within the blastoderm embryo, we observed the RNA and nuclei moving together and we did not detect any particle cycling between apical and basal cytoplasm (Figures 6A–6C; Movie S9). These results suggest a static anchoring of RNA but do not exclude continuous active transport of very small RNA particles, which are below the detection threshold of our microscope. To test this possibility, we photo-bleached a region of apically localized RNA and measured its recovery, a technique known as fluorescence recovery after photo bleaching (FRAP). The continuous active transport model predicts that signal in the photo-bleached regions should be partly restored by delivery of RNAs previously released by the motor and in the process of relocalizing. To test this prediction, we injected green RNA, allowed it to localize, and then photo-bleached a region of localized RNA with a 488 nm laser. Our results show that there is

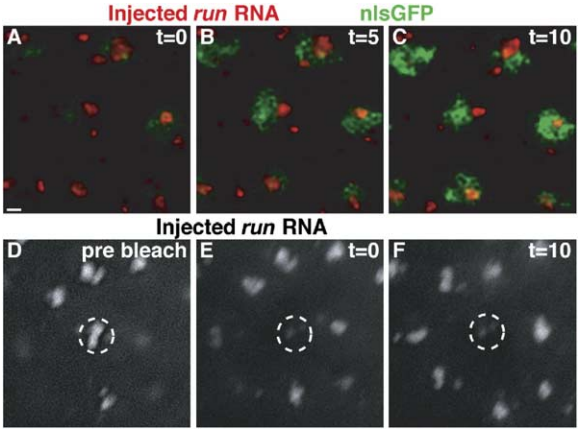

Figure 6. Apical RNA Anchoring Is Static Relative to the Blastoderm Nuclei

(A–C) Apical view of living embryo 15 min after injection of AlexaFluor546-labeled RNA (red), which localizes above the nlsGFP containing nuclei (green). Each image is a projection of ten 1 μm z sections.

(D–F) FRAP experiment. Apical view of living embryo 15 min after injection with AlexaFluor488-labeled RNA. Each image is a projection of ten 1 μm z sections.

(D) Immediately before photo bleaching.

(E) Immediately after photo bleaching one apical patch of RNA (circle).

(F) 10 min after bleaching, there is no recovery of the signal (recovery fraction of 0.0008).

Scale bar is 1 μm.

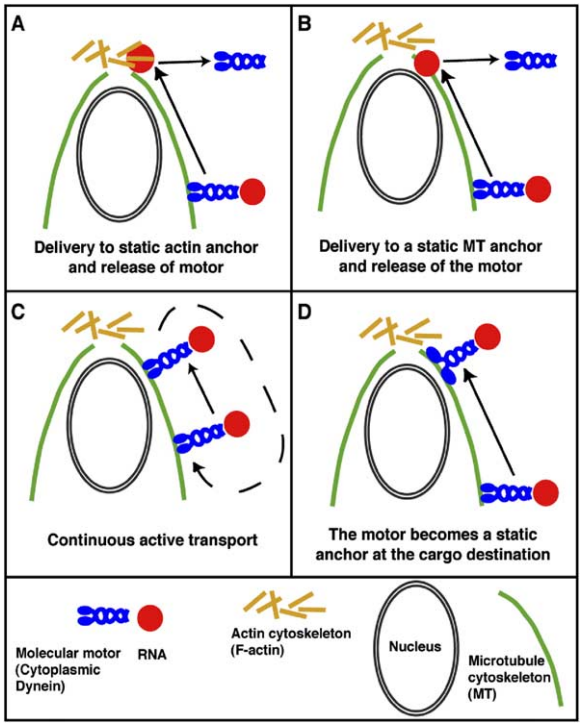

Figure 7. Models for RNA Anchoring

(A–D) There are four main models that could explain how apical mRNAs are retained in the apical cytoplasm after their transport by dynein.

(A) The motor could release the RNA cargo allowing it to attach to an actin-dependent anchor.

(B) The anchor could be MT associated.

(C) Continuous active transport without anchoring could retain the RNA cargo in the apical cytoplasm. After arriving apically, the cargo could detach from the motor, or the motor could detach with the cargo from MTs and then diffuse away. Then the motor-cargo complex would reattach on MTs or the cargo alone recruit a new motor and be transported back to the apical cytoplasm.

(D) The motor could retain the cargo and become a static anchor attached to MTs. Our data support model (D) and argue against the other three models.

no detectable recovery after photo bleaching (Figures 6D–6F). In control experiments, we show that photobleaching the fluorescently tagged RNA does not cause any disruption in the ability of an RNA tagged in another color to move apically (Figure S6). We conclude that there is no continuous flux of RNA to the apical cytoplasm within the limits of resolution of light microscopy. Considering all three lines of analysis described above, we conclude that dynein is not required to continuously transport apical RNA as a means of retaining it in the apical cytoplasm. Instead, once the dynein-RNA complex arrives in the apical cytoplasm, the motor becomes a static anchor and remains colocalized with the cargo.

Discussion

We have used a specific RNA anchoring assay to distinguish between the four main models that could explain how apical *wg* and pair-rule mRNA are retained in the apical cytoplasm after their transport by dynein (Figures 7A–7D). The models we have proposed could also apply to other molecular motors and their various cargos. First, the dynein motor could release the RNA cargo at its final destination, allowing the RNA to bind to an actin-dependent static anchor and the motor to participate in further transport (Figure 7A). Second, the anchor could be MT associated rather than actin based (Figure 7B). Third, RNA could be retained in the apical cytoplasm by continuous active transport without anchoring (Figure 7C). Fourth, the motor itself could retain the cargo and turn into a static anchor when it reaches the final destination (Figure 7D).

At the outset of this study, it was anticipated that cargo anchoring via actin (Figure 7A) was the most likely possibility given that actin is thought to be involved in anchoring of many other RNAs (see Introduction). It was also thought that after a motor completes a transport cycle, it releases the cargo and is available for transport of new cargo. However, in general, there has not been very good direct evidence showing that such a model is correct because of the lack of an assay that could discriminate between the transport and anchoring steps. In our study, we have used two specific assays: one for transport and another for anchoring. We have also been able to assay both anchoring and transport at the same time in the same embryo using two distinct RNAs. These specific assays have allowed us to test and refute the prevailing actin anchoring model at least in the case of pair-rule and *wg* apical mRNA localization in the *Drosophila* blastoderm embryo.

Against expectations, our results show that the fourth model is correct, namely that *wg* and pair-rule RNA are anchored by a dynein-dependent mechanism so that the motor molecules are maintained to the site of anchoring with the cargo. Our data shows that the requirement for dynein to anchor the apical RNA is independent of the ATPase activity of the motor and its transport cofactors Egl and BicD, all of which are required for the active transport of the RNA. These observations are best explained by a model in which the dynein motor involved in apical transport of RNA does not release the cargo and acts as a static anchor at the final destination.

It is interesting to consider how a dynamic motor such as dynein could turn into a static anchor after completion of cargo transport. Dynein is a large multicomplex motor that is difficult to work with in vitro. Nevertheless, many of the subunits of dynein are defined and the force-generating protein, Dhc, is thought to contain physically distinct ATPase and MT binding domains (Gee et al., 1997). It is therefore easy to imagine how the motor could change to a static anchor by remaining attached to MTs via the MT binding domain and losing its ATPase force-generating capacity. Indeed, ATPase-independent MT binding has been observed with dynein under in vitro conditions (Vale et al., 1989). While it is difficult to compare in vitro studies with our studies in vivo, the latter are likely to show much more complex and varied interactions with proteins in the cell. Indeed, anchoring may also involve interactions with additional components not present in vitro, such as MT-associated proteins (MAPs), which could stabilize the binding of dynein to the apical MTs or could physically obstruct the motor movement. Another possibility could be anchoring through association with ribosomes, but this can be ruled out in the case of *wg* and pair-rule RNA, since RNAs lacking a coding region can be transported and anchored correctly (R.D. and I.D., unpublished data). Alternative hypotheses, which cannot be ruled out, include a change of conformation or modifications of the structure of the dynein-dynactin complex. While our data demonstrate conclusively a new RNA-anchoring function for dynein, they do not allow us to distinguish between the various hypotheses of how this anchoring occurs at the molecular level, nor test definitively whether Dynactin is required for anchoring. We show that p50/dynamitin is present with the anchored RNA and that overexpression of p50/dynamitin and a Glued/p150 allele cause a partial inhibition of RNA localization with no obvious effects on anchoring. These results suggest, but do not demonstrate conclusively, that Dynactin is not required for anchoring. Furthermore, while we show that the ATPase activity of the motor is not required for anchoring, this observation does not test whether dynactin is required in addition to dynein for anchoring.

Whatever the molecular basis for the dynein anchoring function we have uncovered, it seems likely that the anchoring which we describe does not involve a single dynein molecule anchoring a single RNA molecule. Instead, the RNA cargo is likely to consist of particles containing many RNA molecules (Wilkie and Davis, 2001) and probably many motor complexes. The cargo is thus likely to remain strongly attached to at least some motor molecules throughout transport and anchoring. However, it is not yet known what the linkers between the RNA and motors are (Tekotte and Davis, 2002).

Little is also known about the mechanism of anchoring of other dynein cargos, although the mechanism of transport of RNA by dynein could be very similar to other cargos such as lipid droplets (Welte et al., 1998). Dynein is also required for nuclear positioning and tethering in many systems (Morris, 2003), so its role as a static anchor may be widespread. Furthermore, some kinesin-like proteins are also thought to interact with static cell components (Maddox et al., 2003), and recent in vitro studies show that myosin VI can switch from a motor to an anchor under tension (Altman et al., 2004; Miller, 2004). This process has been proposed to stabilize actin cytoskeletal structures and link protein complexes to actin structures (Miller, 2004). We therefore propose that myosins, kinesins, and dynein may all be able to switch under certain circumstances from dynamic motors to static anchors and that our observations may represent a general principle for anchoring of some cargos following transport to their final cytoplasmic destination.

Experimental Procedures

Fly Strains

Stocks were raised on standard cornmeal-agar medium at 25°C. Injections were into wild-type (Oregon R) embryos or a strain with four copies of an *nls-GFP* transgene (*yw*; *nls-GFPM*; *nls-GFPN*) (Davis et al., 1995). *Dhc64C* mutants were from T. Hays (Gepner et al., 1996). γ-*Tubulin37C*^{1}/γ-*Tubulin37C*^{3} and *Glued*^{1} were from the Bloomington Stock Center. *BicD*^{H40}/*BicD*^{R26}, *BicD*^{H3}/*BicD*^{R26}, *egl*^{3e}/*egl*^{WU50} were from R. Lehann and Oh et al. (2000). *UAS human dynamitin* (A. Guichet) was overexpressed using the *NGT40 GAL4* driver (Tracey et al., 2000).

RNA Anchoring Assay

Embryos were prepared for injection; capped RNAs were transcribed in vitro and injected as previously described, at concentrations of 250–500 ng/μl (Wilkie and Davis, 2001). In some experiments, injection of DMSO, LatrunculinA (10 mM; Sigma), Colcemid (100 μg/ml; Sigma), Nocodazole (10 μM; Sigma), sodium orthovanadate (Sigma) at 10 mM, anti-Dhc antibody (Sharp et al., 2000), anti-Dic (clone 74.1, Chemicon), anti-Egl (R. Lehmann), anti-BicD (clone 4C2, B. Suter) (Suter and Steward, 1991), control anti-Notch (DSHB), anti-GFP (Molecular Probes), and anti-β-Galactosidase (Promega) were injected after complete apical localization of injected fluorescently labeled RNAs. Injection dilutes the reagent 50–100 times (Edgar et al., 1987). Colcemid and Nocodazole were injected in early cycle 14, since MTs are more stable at later times (data not shown). Injection of Vanadate partly disorganized the MTs by removing F-actin structures (data not shown). To inhibit active transport, embryos were preinjected with Vanadate or anti-Egl antibody 10 min before the fluorescent RNA injections.

RNA In Situ Hybridization and Immunofluorescence

In situ hybridization and fluorescent detection by tyramide signal amplification (Perkin Elmer) were carried out as previously described (Wilkie and Davis, 2001). In RNA and F-actin colocalization experiments, embryos were devitellinized by hand-peeling and stained with FITC or AlexaFluor568-coupled phalloidin (Molecular Probes; Foe et al., 2000), followed by the in situ hybridization procedure, causing degradation of the quality of F-actin staining. For covisualization of injected RNA and F-actin, Biotin-labeled RNA was detected with Avidin AlexaFluor568 (Molecular Probes). AlexaFluor488 wheat germ agglutinin (Molecular Probes) was used

to visualize the nuclear envelope. Anti-Egl (R. Lehmann) and Anti-BicD (1B11 B. Suter) were used at 1/4000 and 1/20, respectively. Rabbit anti-Dhc antibody (PEP1, T. Hays; Li et al., 1994) was used at 1/300 and mouse anti-p50/dynamitin antibody at 1/250 (clone 25, BD Biosciences). For optimal MT preservation, injected or uninjected embryos were dechorionated then shaken in 1:1 heptan/methanol, 0.15 M EGTA, and then incubated in Methanol 0.15 M EGTA for at least 4 hr at −20°C, rehydrated in 20%, 40%, 60%, 80%, and 100% PBS in methanol and postfixed in 3.7% formaldehyde in PBS, 0.1% Tween (PBT) for 20 min.

After several washes in PBT, in situ hybridization was carried out as above. MTs were detected by incubating overnight at 4°C with a mouse anti-α-tubulin-FITC (1/1000; Sigma) and centrosomes by a rabbit anti-Cnn antibody (1/1000, T. Kaufmann; Megraw et al., 2002) or a mouse anti-γ-tubulin antibody (1/1000; Sigma). Secondary antibodies used were AlexaFluor488, AlexaFluor568 (Molecular probes), or Cy5 (Jackson) conjugated. DNA was labeled with DAPI.

Imaging and FRAP Analysis

Fixed embryos were mounted in Vectashield (Vector Laboratories) and living embryos were imaged directly on coverslips in halocarbon oil (Davis, 2000). Imaging was performed on a widefield DeltaVision microscope (Applied Precision, Olympus IX70 and Roper Coolsnap HQ). Images were acquired with 10×/0.4 NA, 20×/0.75 NA, or 100×/1.4 NA and then deconvolved. Up to ten living embryos were imaged in parallel. Photo-bleaching experiments used a 488 nm laser line with 12 iterations at the maximum intensity and measurement of the recovery of the fluorescence initiated 1 s later, analyzed using SoftWorx Explorer (Applied Precision) and plotted using Microsoft Excel. Confocal imaging of the anti-Dhc staining were performed on a Leica TCS SP microscope.

Supplemental Data

Supplemental Data include six figures, one table, and nine movies and can be found with this article online at http://www.cell.com/cgi/content/full/122/1/97/DC1/.

Acknowledgments

We thank Adrian Bird, Jean Beggs, William Earnshaw, David Tollervey, Robin Alshire, Catherine Rabouille, Andreas Merdes, Simon Bullock, and Davis lab members for discussions and comments on the manuscript; Paul Taylor and Richard Parton for help with imaging and computer infrastructure. We are also grateful to John Scholey, David Sharp, Tom Hays, Thom Kaufman, Beat Sutter, Ruth Lehmann, David Ish-Horowicz, Simon Bullock, and the Bloomington *Drosophila* Stock Center for antibodies and fly stocks. This work was supported by a Wellcome Trust senior research fellowship (067413) to I.D. and by a Marie Curie fellowship to R.D.

Received: November 19, 2004
Revised: March 4, 2005
Accepted: April 28, 2005
Published: July 14, 2005

References

Altman, D., Sweeney, H.L., and Spudich, J.A. (2004). The mechanism of myosin VI translocation and its load-induced anchoring. Cell *116*, 737–749.

Babu, K., Cai, Y., Bahri, S., Yang, X., and Chia, W. (2004). Roles of Bifocal, Homer, and F-actin in anchoring *oskar* to the posterior cortex of *Drosophila* oocytes. Genes Dev. *18*, 138–143.

Beach, D.L., Salmon, E.D., and Bloom, K. (1999). Localization and anchoring of mRNA in budding yeast. Curr. Biol. *9*, 569–578.

Bertrand, E., Chartrand, P., Schaefer, M., Shenoy, S.M., Singer, R.H., and Long, R.M. (1998). Localization of *ASH1* mRNA particles in living yeast. Mol. Cell *2*, 437–445.

Brendza, R.P., Serbus, L.R., Duffy, J.B., and Saxton, W.M. (2000). A function for kinesin I in the posterior transport of *oskar* mRNA and Staufen protein. Science *289*, 2120–2122.

Bullock, S.L., and Ish-Horowicz, D. (2001). Conserved signals and machinery for RNA transport in *Drosophila* oogenesis and embryogenesis. Nature *414*, 611–616.

Bullock, S.L., Stauber, M., Prell, A., Hughes, J.R., Ish-Horowicz, D., and Schmidt-Ott, U. (2004). Differential cytoplasmic mRNA localisation adjusts pair-rule transcription factor activity to cytoarchitecture in dipteran evolution. Development *131*, 4251–4261.

Callaini, G., and Anselmi, F. (1988). Centrosome splitting during nuclear elongation in the *Drosophila* embryo. Exp. Cell Res. *178*, 415–425.

Davis, I. (2000). Visualising fluorescence in *Drosophila*—optimal detection in thick specimens. In Protein Localisation by Fluorescence Microscopy: A Practical Approach, V.J. Allan, ed. (Oxford: Oxford University Publishing), pp. 131–162.

Davis, I., and Ish-Horowicz, D. (1991). Apical localization of pair-rule transcripts requires 3′ sequences and limits protein diffusion in the *Drosophila* blastoderm embryo. Cell *67*, 927–940.

Davis, I., Girdham, C.H., and O'Farrell, P.H. (1995). A nuclear GFP that marks nuclei in living *Drosophila* embryos—maternal supply overcomes a delay in the appearance of zygotic fluorescence. Dev. Biol. *170*, 726–729.

Duncan, J.E., and Warrior, R. (2002). The cytoplasmic Dynein and Kinesin motors have interdependent roles in patterning the *Drosophila* oocyte. Curr. Biol. *12*, 1982–1991.

Edgar, B.A., Odell, G.M., and Schubiger, G. (1987). Cytoarchitecture and the patterning of *fushi tarazu* expression in the *Drosophila* blastoderm. Genes Dev. *1*, 1226–1237.

Erdelyi, M., Michon, A.M., Guichet, A., Glotzer, J.B., and Ephrussi, A. (1995). Requirement for *Drosophila* cytoplasmic tropomyosin in *oskar* mRNA localization. Nature *377*, 524–527.

Ferrandon, D., Elphick, L., Nüsslein-Volhard, C., and St Johnston, D. (1994). Staufen protein associates with the 3′UTR of *bicoid* mRNA to form particles that move in a microtubule-dependent manner. Cell *79*, 1221–1232.

Foe, V.E., Odell, G.M., and Edgar, B.A. (1993). Mitosis and morphogenesis in the *Drosophila* embryo: Point and counterpoint. In The Development of *Drosophila melanogaster*, M. Bate and A. Martinez-Arias, eds. (New York: Cold Spring Harbor Laboratory Press), pp. 149–300.

Foe, V.E., Field, C.M., and Odell, G.M. (2000). Microtubules and mitotic cycle phase modulate spatiotemporal distributions of F-actin and myosin II in Drosophila syncytial blastoderm embryos. Development *127*, 1767–1787.

Gee, M.A., Heuser, J.E., and Vallee, R.B. (1997). An extended microtubule-binding structure within the dynein motor domain. Nature *390*, 636–639.

Gepner, J., Li, M., Ludmann, S., Kortas, C., Boylan, K., Iyadurai, S.J., McGrail, M., and Hays, T.S. (1996). Cytoplasmic dynein function is essential in *Drosophila melanogaster*. Genetics *142*, 865–878.

Glotzer, J.B., Saffrich, R., Glotzer, M., and Ephrussi, A. (1997). Cytoplasmic flows localize injected *oskar* RNA in *Drosophila* oocytes. Curr. Biol. *7*, 326–337.

Gonzalez-Reyes, A., Elliott, H., and St Johnston, D. (1995). Polarization of both major body axes in *Drosophila* by Gurken-Torpedo signaling. Nature *375*, 654–658.

Gordon, J.A. (1991). Use of vanadate as protein-phosphotyrosine phosphatase inhibitor. Methods Enzymol. *201*, 477–482.

Hoogenraad, C.C., Akhmanova, A., Howell, S.A., Dortland, B.R., De Zeeuw, C.I., Willemsen, R., Visser, P., Grosveld, F., and Galjart, N. (2001). Mammalian Golgi-associated Bicaudal-D2 functions in the dynein-dynactin pathway by interacting with these complexes. EMBO J. *20*, 4041–4054.

Jankovics, F., Sinka, R., Lukacsovich, T., and Erdelyi, M. (2002). MOESIN crosslinks actin and cell membrane in *Drosophila* oocytes and is required for *oskar* anchoring. Curr. Biol. *12*, 2060–2065.

Januschke, J., Gervais, L., Dass, S., Kaltschmidt, J.A., Lopez-Schier, H., St Johnston, D.S., Brand, A.H., Roth, S., and Guichet, A.

(2002). Polar transport in the *Drosophila* oocyte requires Dynein and Kinesin I cooperation. Curr. Biol. *12*, 1971–1981.

Kanai, Y., Dohmae, N., and Hirokawa, N. (2004). Kinesin transports RNA: Isolation and characterization of an RNA-transporting granule. Neuron *43*, 513–525.

Lambert, J.D., and Nagy, L.M. (2002). Asymmetric inheritance of centrosomally localized mRNAs during embryonic cleavages. Nature *420*, 682–686.

Latham, V.M., Yu, E.H., Tullio, A.N., Adelstein, R.S., and Singer, R.H. (2001). A Rho-dependent signaling pathway operating through myosin localizes beta-actin mRNA in fibroblasts. Curr. Biol. *11*, 1010–1016.

Li, M., McGrail, M., Serr, M., and Hays, T.S. (1994). *Drosophila* cytoplasmic dynein, a microtubule motor that is asymmetrically localized in the oocyte. J. Cell Biochem. *126*, 1475–1494.

Lopez de Heredia, M., and Jansen, R.P. (2004). mRNA localization and the cytoskeleton. Curr. Opin. Cell Biol. *16*, 80–85.

MacDougall, N., Clark, A., MacDougall, E., and Davis, I. (2003). *Drosophila gurken* (TGFα) mRNA localizes as particles that move within the oocyte in two dynein-dependent steps. Dev. Cell *4*, 307–319.

Mach, J.M., and Lehmann, R. (1997). An Egalitarian-BicaudalD complex is essential for oocyte specification and axis determination in *Drosophila*. Genes Dev. *11*, 423–435.

Maddox, P.S., Stemple, J.K., Satterwhite, L., Salmon, E.D., and Bloom, K. (2003). The minus end-directed motor Kar3 is required for coupling dynamic microtubule plus ends to the cortical shmoo tip in budding yeast. Curr. Biol. *13*, 1423–1428.

Matanis, T., Akhmanova, A., Wulf, P., Del Nery, E., Weide, T., Stepanova, T., Galjart, N., Grosveld, F., Goud, B., De Zeeuw, C.I., et al. (2002). Bicaudal-D regulates COPI-independent Golgi-ER transport by recruiting the dynein-dynactin motor complex. Nat. Cell Biol. *4*, 986–992.

Megraw, T.L., Kilaru, S., Turner, F.R., and Kaufman, T.C. (2002). The centrosome is a dynamic structure that ejects PCM flares. J. Cell Sci. *115*, 4707–4718.

Miller, K.G. (2004). Converting a motor to an anchor. Cell *116*, 635–636.

Morris, N.R. (2003). Nuclear positioning: the means is at the ends. Curr. Opin. Cell Biol. *15*, 54–59.

Navarro, C., Puthalakath, H., Adams, J.M., Strasser, A., and Lehmann, R. (2004). Egalitarian binds dynein light chain to establish oocyte polarity and maintain oocyte fate. Nat. Cell Biol. *6*, 427–435.

Neuman-Silberberg, F.S., and Schüpbach, T. (1993). The *Drosophila* dorsoventral patterning gene *gurken* produces a dorsally localized RNA and encodes a TGFα-like protein. Cell *75*, 165–174.

Oh, J., Baksa, K., and Steward, R. (2000). Functional domains of the *Drosophila* bicaudal-D protein. Genetics *154*, 713–724.

Palacios, I.M., and St Johnston, D.S. (2001). Getting the message across: the intracellular localization of mRNAs in higher eukaryotes. Annu. Rev. Cell Dev. Biol. *17*, 569–614.

Palacios, I.M., and St Johnston, D.S. (2002). Kinesin light chain-independent function of the Kinesin heavy chain in cytoplasmic streaming and posterior localisation in the *Drosophila* oocyte. Development *129*, 5473–5485.

Schnorrer, F., Bohmann, K., and Nüsslein-Volhard, C. (2000). The molecular motor dynein is involved in targeting swallow and *bicoid* RNA to the anterior pole of *Drosophila* oocytes. Nat. Cell Biol. *2*, 185–190.

Schnorrer, F., Luschnig, S., Koch, I., and Nusslein-Volhard, C. (2002). γ-*Tubulin37C* and γ-*tubulin ring complex protein 75* are essential for *bicoid* RNA localization during *Drosophila* oogenesis. Dev. Cell *3*, 685–696.

Sharp, D.J., Rogers, G.C., and Scholey, J.M. (2000). Cytoplasmic dynein is required for poleward chromosome movement during mitosis in *Drosophila* embryos. Nat. Cell Biol. *2*, 922–930.

Simmonds, A.J., dosSantos, G., Livne-Bar, I., and Krause, H.M. (2001). Apical localization of *wingless* transcripts is required for wingless signaling. Cell *105*, 197–207.

St Johnston, D., Driever, W., Berleth, T., Richstein, S., and Nüsslein-Volhard, C. (1989). Multiple steps in the localization of *bicoid* RNA to the anterior pole of the *Drosophila* oocyte. Development *107*, 13–19.

Steffen, W., Karki, S., Vaughan, K.T., Vallee, R.B., Holzbaur, E.L., Weiss, D.G., and Kuznetsov, S.A. (1997). The involvement of the intermediate chain of cytoplasmic dynein in binding the motor complex to membranous organelles of *Xenopus* oocytes. Mol. Biol. Cell *8*, 2077–2088.

Stephenson, E.C., Chao, Y.C., and Fackelthal, J.D. (1988). Molecular analysis of the *swallow* gene of *Drosophila melanogaster*. Genes Dev. *2*, 1655–1665.

Sundell, C.L., and Singer, R.H. (1991). Requirement for microfilaments in sorting of actin messenger RNA. Science *253*, 1275–1277.

Suter, B., and Steward, R. (1991). Requirement for phosphorylation and localization of the Bicaudal-D protein in *Drosophila* oocyte differentiation. Cell *67*, 917–926.

Takizawa, P.A., Sil, A., Swedlow, J.R., Herskowitz, I., and Vale, R.D. (1997). Actin-dependent localization of an RNA encoding a cell-fate determinant in yeast. Nature *389*, 90–93.

Tekotte, H., and Davis, I. (2002). Intracellular mRNA localization: motors move messages. Trends Genet. *18*, 636–642.

Tracey, W.D., Jr., Ning, X., Klingler, M., Kramer, S.G., and Gergen, J.P. (2000). Quantitative analysis of gene function in the *Drosophila* embryo. Genetics *154*, 273–284.

Vale, R.D. (2003). The molecular motor toolbox for intracellular transport. Cell *112*, 467–480.

Vale, R.D., Soll, D.R., and Gibbons, I.R. (1989). One-dimensional diffusion of microtubules bound to flagellar dynein. Cell *59*, 915–925.

Van de Bor, V., and Davis, I. (2004). mRNA localisation gets more complex. Curr. Opin. Cell Biol. *16*, 300–307.

Wagner, C., Palacios, I., Jaeger, L., St Johnston, D., Ehresmann, B., Ehresmann, C., and Brunel, C. (2001). Dimerization of the 3′UTR of *bicoid* mRNA involves a two-step mechanism. J. Mol. Biol. *313*, 511–524.

Welte, M.A., Gross, S.P., Postner, M., Block, S.M., and Wieschaus, E.F. (1998). Developmental regulation of vesicle transport in *Drosophila* embryos: Forces and kinetics. Cell *92*, 547–557.

Wilkie, G.S., and Davis, I. (2001). *Drosophila wingless* and pair-rule transcripts localize apically by dynein-mediated transport of RNA particles. Cell *105*, 209–219.

Yisraeli, J.K., Sokol, S., and Melton, D.A. (1990). A two-step model for the localization of maternal mRNA in *Xenopus* oocytes: involvement of microtubules and microfilaments in the translocation and anchoring of *Vg1* mRNA. Development *108*, 289–298.